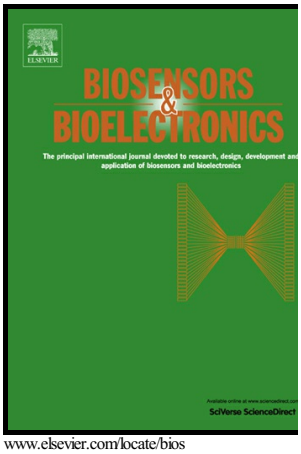

www.elsevier.com/locate/bios

Current trends in nanomaterial embedded field effect transistor-based biosensor

Anuj Nehra, Krishna Pal Singh

PII: S0956-5663(15)30275-X
DOI: http://dx.doi.org/10.1016/j.bios.2015.07.030
Reference: BIOS7848

To appear in: *Biosensors and Bioelectronic*

Received date: 8 May 2015
Revised date: 7 July 2015
Accepted date: 14 July 2015

Cite this article as: Anuj Nehra and Krishna Pal Singh, Current trends i nanomaterial embedded field effect transistor-based biosensor, *Biosensors an Bioelectronic,* http://dx.doi.org/10.1016/j.bios.2015.07.030

Review

Current trends in nanomaterial embedded field effect transistor-based biosensor

Anuj Nehra [a,1], Krishna Pal Singh [b,2]

[a]*Nanobiotechnology Research Laboratory, Centre of Excellence for Mountain Biology, Uttarakhand Council for Biotechnology, Biotech Bhavan, Haldi-263146, U. S. Nagar, Uttarakhand, India*

[b]Bio-Nanotechnology Research Laboratory, Biophysics Unit ,CBSH, G.B. Pant University of Agriculture & Technology, Pantnagar-263145, U.S Nagar, Uttarakhand, India

Abstract

Recently, as metal-, polymer-, and carbon-based biocompatible nanomaterials have been increasingly incorporated into biosensing applications, with various nanostructures having been used to increase the efficacy and sensitivity of most of the detecting devices, including field effect transistor (FET)-based devices. These nanomaterial-based methods also became the ideal for the amalgamation of biomolecules, especially for the fabrication of ultrasensitive, low-cost, and robust FET-based biosensors; these are categorically very successful at binding the target specified entities in the confined gated micro-region for high functionality. Furthermore, the contemplation of nanomaterial-based FET biosensors to various applications encompasses the desire for detection of many targets with high selectivity, and specificity. We assess how such devices have empowered the achievement of elevated biosensor performance in terms of high sensitivity, selectivity and low detection limits. We review the recent literature here to illustrate the diversity of FET-based biosensors, based on various kinds of nanomaterials in different applications and sum up that graphene or its assisted composite based FET devices are comparatively more efficient and sensitive with highest signal to noise ratio. Lastly, the future prospects and limitations of the field are also discussed.

Highlights

►The uses of various nanomaterials in FET-based biosensors are reviewed.
►Graphene-based FET biosensor could be able to easily detect various biomolecules, such as proteins, polysaccharides, cytochrome-c, lipids, NADH, hemoglobin, HRP, nucleic acids, and small molecules, such as primary metabolites, secondary metabolites, and natural products.
►The large surface area and good sensitivity of graphene based nanomaterial in conjunction with polymeric matrices seems to be more beneficial for detecting different biomolecules.

Keywords: Nanobiosensors, nanomaterial, nanotechnology, biocompatible, graphene

1. Introduction

Among the silicon-based biosensors, the field effect transistor (FET) based on ion selectivity (ISFET) is considered the most popular electric biosensor due to its sensitivity, speed, miniaturization, and low cost and because it can detect pH, penicillin, DNA, proteins, enzymes, and cells (Bergveld et al., 1970; Caras and Janata, 1980; Yuqing et al., 2003; Lee et al, 2009). The label-free FET biosensors have recently attracted a great deal of attention due to the incorporation of various biocompatible nanomaterials on its exposed micro region gate to enhance its sensitivity and selectivity.

Nanomaterials include a diverse range of materials, such as inter alia inorganic metal, metal oxide, polymeric particulate materials, and organic materials (Schwirn et al., 2014) in forms that are important in nanoscience and nanotechnology. A broad range of nanomaterials, such as carbon nanotubes, graphene, nanocomposites, nanofibers, nanoparticles, nanowires (NWs), quantum dots, nanorods, nanofilms, and nanopores, are being employed in drug delivery systems, novel robotic devices, molecule-by-molecule design, self-assembly structure, and biosensing, and new uses of these materials are being discovered by the day (Schwirn et al., 2014). The tunable and unique properties of nanomaterials offer excellent interfacing prospects for biological identification, even with electronic signal transduction for designing new bioelectronics devices that exhibit novel functions.

We will discuss here the most important classes of nanomaterials for biosensing purposes. These nanomaterials possess novel properties in one or other form for biosensor arrays because of their high chemical adjustability, easy synthesis, and broad integration into detection devices to enhance

[1] *The author contributed equally in this work*

[2] *Corresponding author at: Bio-Nanotechnology Research Laboratory, Biophysics Unit, CBSH, G.B Pant University of Agriculture & Technology, Pantnagar-263145, U.S Nagar, Uttarakhand, India.*
Tel.: +91 9412632572; fax: +91 5944 233473
Email address: kps_biophysics@yahoo.co.in (K. P. Singh)

sensitivity and efficacy to target analytes. In general, nanomaterials-based biosensors are called nanobiosensors and have very fast responses, small size, and high sensitivity and portability (Yun et al., 2009). Newer nanomaterials with good conductivity, high strength, and nanoscale size are being employed in the detection of biological molecules, up to the lower limits of various sensing devices (Fan et al., 2008; Khanna, 2008; Velasco, 2009; You et al., 2009). Among the various kinds of biosensors that are classified by the mode of physicochemical signal transduction (Thevenot et al., 1999), field effect transistor (FET)-based biosensors are a new class of sensing device; FET-based biosensors are cheap and allow the analysis of species with great specificity, rapidity, sensitivity, and high selectivity (Law et al., 2015; Koppenhöfer et al., 2015; Wustoni et al., 2015).

Recently, many kinds of nanomaterials, such as carbon nanotubes (Balasubramanian and Burghard, 2006), nanoparticles (Holzinger et al., 2014), optical fibre, and graphene-based materials (Artiles et al., 2011; Tian et al., 2014) were continuously used in the fabrication of FET-based biosensors and have prominence in terms of sensitivity and easy fabrication, relative to other biosensing devices. The FET-based biosensor gives an interesting platform for analysing the content of biological fragments because of the direct conversion of biological action into electronic signals, which can be the shortest route of detection. Therefore, development of quick, valuable, and label-free FET-based biosensors drew attention (Sarkar et al., 2014) among recent biosensing devices.

In this review, we will focus on: how the various biocompatible nanomaterials used in FET-based biosensors are utilised; their description, applications, and challenges; comparing them by detection limit; and their response time and signal to noise ratio (SNR).

2. FET-based Biosensor

The first three-electrode structure containing the drain, source, and gate, shown schematically in Figure.1A, was established 1970 as an ISFET (Bergveld, 1970), and was used to detect penicillin by the enzymatic modification of the gate (Caras and Janata, 1980). Currently, great progress has been achieved for ISFET biosensors regarding the amount of biomolecules on the dielectric gate, pH, variety of incorporated ions, enzymatic reaction products, and other factors. ISFET is categorized by the various biological elements used: enzyme FET, DNA FET, and immuno-FET, which incorporate layers of immobilized enzymes, DNA strands, and antibodies, respectively (Janata and Moss, 1976; Schasfoort et al., 1990; Fromherz et al., 1991; Wolf et al., 1998; Zayats et al., 2000; Zayats et al., 2002).

Recently, Wustoni et al. demonstrated a FET-based biosensor for the detection of a human prion protein, using thiamine as a probe molecule. This fabricated sensor was designed according to the dual-ligand binding of metal ions (Cu^{2+}) and prion protein on the thiamine-immobilized surface due to extra positive charge induced on the gate surface of the FET. The achieved detection limit of the prion proteins was very low (i.e., >2 nM) with concentration of 40 pM- 40 nM (Wustoni et al., 2015). Law et al. reported that a FET-based sensor monitored human T cells by impedance spectrometry and studied adhesion strengths and migration of single-cells (human $CD8^+$ T) on a pre-coated (i.e., 0.1 mg/ml fibronectin, anti-CD3 antibody, and anti-LFA-1 antibody) gate micro region. In this sensor, the seal resistance (R_{seal}) created between the gate surface and cellular membrane and the combined membrane capacitance (C_M) were acquired for every adhesion phenomenon. Further, R_{seal} was used to detect the adhesion strength between the fibronectin and cells, while was C_M employed to detect the morphology of the adhered cells' alteration in event adhesion (Law et al., 2015). Koppenhöfer et al. suggested a new FET-based biosensor using electrical cell-substrate impedance sensing (ECIS) for the detection of apoptosis-generating events of hydrogen peroxide analysis on primary cells from the subventricular zone of postnatal BALB/c mice. Upon cell death, the cell-substrate adhesions of the neurons are evenly tired until completed disconnection (Koppenhöfer et al., 2015).

An aptamer modified FET biosensor was developed by Goda and Miyahara for the detection of thrombin and lysozyme. In this sensor, an Au electrode is extended to the gate of the FET-, because protein can be covalently immobilized on the Au electrode with thiol molecules and then made into a closely packed, self-assembled monolayer. The charge carriers are exchanged at the gate/solution interface for specific protein binding-, because of the intrinsic total charge of the captured protein. This biosensor successfully determined the thrombin and lysozyme concentrations within the ranges of 15.2-1040 nM and 13.4-1300 nM, respectively (Goda and Miyahara, 2013).

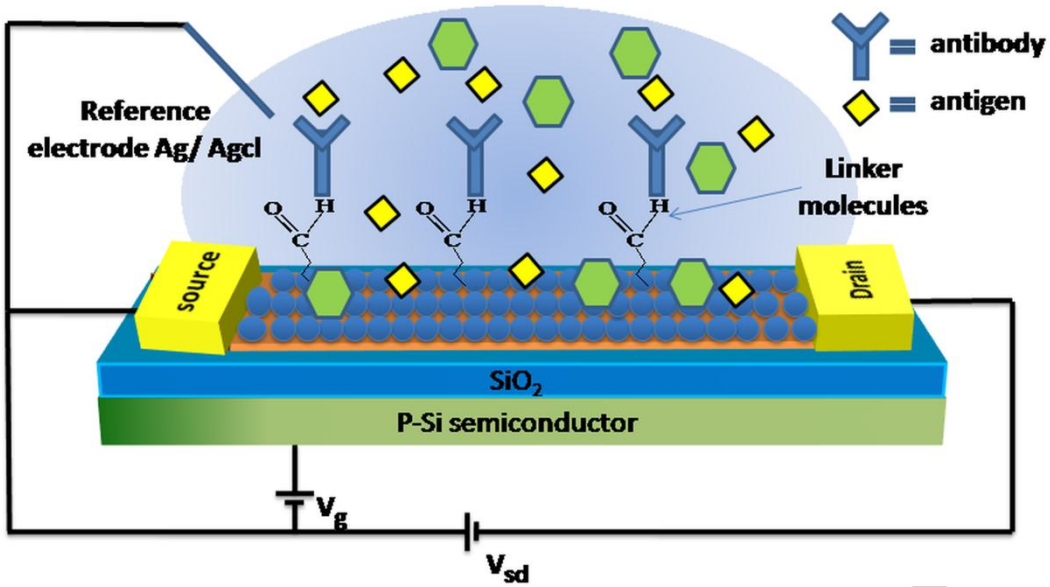

Fig.1 A. Schematic diagram of a FET-based biosensor.

3. Nanomaterials in FET-based biosensors

Nanomaterials attracted the attention of scientists since its inception (Gleiter, 1989) and through the invention of graphene (Geim and Novoselov, 2007) for their employment in various application including biosensing devices. Different nanomaterials, such as magnetic nanoparticles, silicon NW, titanium dioxide, zinc oxide, gallium nitride, carbon nano tubes, and graphene have been used by various workers for the dielectric gates of FET-based biosensors (Figure.1B).

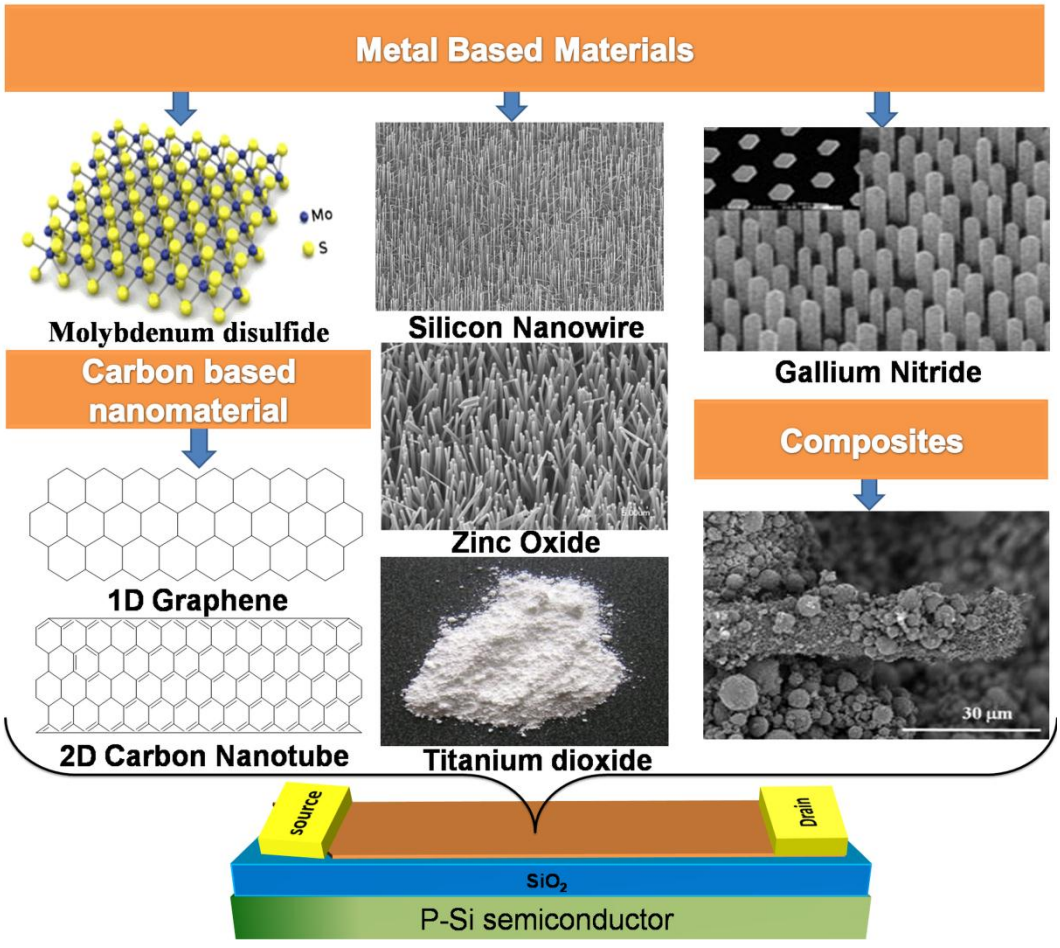

Fig.1 B. Different nanomaterials embedded onto the gated region of the FET-based biosensor shown in Figure 1 A.

3.1 Magnetic nanoparticle-based FET biosensors

Magnetic nanoparticles (MNPs) have many exclusive magnetic properties, including high coercivity, super paramagnetism, high magnetic susceptibility, and low Curie temperature. Researchers from a wide range of disciplines, including magnetic fluids, data storage, catalysis, and bio-applications prefer these nanomaterials (Patel et al., 2008; Zhao et al., 2003; Mornet et al., 2006; Stevens et al., 2005; Jun et al., 2007). They are formed from the magnetic component as nickel, cobalt, iron, and their oxides like cobalt ferrite (Fe_2CoO_4), maghemite (γ –Fe_2O_3), chromium dioxide (CrO_2), and magnetite (Fe_3O_4) (Indira and Lakshmi, 2010). The first deliberate development of magnetic fluid was presented by Elmore in the late 1930s (Elmore, 1938). The first use of MNPs for biomedical purposes (hyperthermia treatment) was carried out in 1957, when different tissue samples were heated with 20 to 100 nm γ-Fe_2O_3 disclosed to a 1.2 MHz magnetic field (Gilchrist et al., 1957). MNPs also allow label-free biosensing (Shen et al., 2008; Lowery et al., 2008). Furthermore, the MNPs-based biosensing methods support smaller background noise, because there is insufficient or no magnetic signal from biological molecules (Haun et al., 2010; Shao et al., 2012). Recently, MNPs have used in development of the enzyme FET for estimation of triglycerides. This device has enabled to estimate the triglyceride concentrations in the range of 0.1–1.5% by immobilizing a thermostable lipase on nanoparticles (Vijayalakshmia et al., 2008).

Table.1
Comparative study of various types of nanomaterial based-FET biosensors

Sensors	Nanomaterials	Detection limit	Sensitivity[a] /RSD (%)&(S/N)[b]/ Response time[c]/ Transconductance[d]	Range	Detection mode	Detection	Reference
pH sensor	Graphene	0.025	[b] (S/N=3)	4.04 - 8.16	CDC at DSV 0.1V	pH value	Ohno et al. (2010a)
	3 bilayers of (PVS)/(N-PANI) onto the Au substrate	_	[a] 58mVpH^{-1}/ [c]180 s	2 - 12	CDSV	pH value	Vieira et al. (2011)
	Dendrimer/TiO_2-nanoparticle	_	[a]57 mVpH^{-1}/ [c]180 s	4 - 10	CDSV	pH value	Vieira et al. (2012)
	TiO_2/ITO glass	_	[a]42.1 mVpH^{-1}	4 - 10	CDS	pH value	Rosdan et al. (2013)
	TiO nanorods (NR)	_	[a]49.6 mVpH^{-1}	2 - 12	CDS	pH value	Guerra and Mulato (2014)
	Molybdenum disulfide (MoS_2)	_	[a] 59 mVpH^{-1} (713) pH change 1 unit	3 - 9	CDC	pH value	Sarkar et al. (2014)
	Single-wall CNT	_	_	5 - 9	CDC	pH value	Kiani et al. (2015)
Glucose sensors	CPNT	_	[a]1.7/ [c]5 –10 s	0.5 -20 mM	CDC	Glucose	Yoon et al. (2008)
	CVD-Graphene	0.1 mM	[b] 0.16	0.1mM - 10mM	CDC	Glucose	Huang et al. (2010)
	CVD-Graphene	5 µM	[b] 0.08	5 µM - 0.4 mM	CDC	Glutamate	Huang et al. (2010)
	CNT with PET modified by analytical modeling	_	[a]18.75 A/mM	2 – 10 mM	CDC	Glucose	Pourasl et al. (2014)
	CPNT wrapped graphene sheet	1 nM	[b] (S/N=3.22)/ [c]< 1 s	1 nM - 100 mM	CDC	Glucose	Park et al. (2015)
	Modified graphene with PtNPs with Nafion and chitosan (CHIT)	> 0.5 µM	[d]2 mS	0.5 µM – 1 mM	CDC	Glucose	Zhang et al. (2015)

DNA sensors	Gallium nitride (GaN) nanowire	1 aM	–	1 aM – 10 nM	CDC	Deoxyribonucleic acid (DNA)	Chen et al. (2011)
	Reduced graphene oxide	> 100 fM	[a]100 fM	10 fM - 1nM	CDC	Peptide nucleic acid-DNA hybridization	Cai et al. (2014)
	CVD graphene	8 pM	_	50 pM – 300 pM	CDC	DNA	Kakatkar et al. (2015)
Protein sensors	SWNT by modified Schottky-contact area	1 pM	_	1 nM – 1 pM	CDC	Non specific protein-A staphylococcus aureus (SpA), streptavidin (SA)	Byon and Choi (2006)
		1 pM	_	1 nM - 1 pM	CDC	Specific protein (IgG and anti β-hCG)	Byon and Choi (2006)
	Graphene	_	[d] Conductance and mobility increased	80 nM and 100 nM	CDC	Bovine serum albumin (BSA)	Ohno et al. (2010a)
	TRGO with AuNPs	~ 13 pM	_	2 ng/mL – 0.02 mg/mL	CDC	Protein (IgG)	Mao et al. (2010)
	Titanium dioxide (TiO_2) nanowire	-3.96 A/(ng/mL) at 5 V and R- square = 0.903	_	119 pg/mL – 5.95 ng/mL	CDC	Protein rabbit IgG at the nano-gram level	Chu et al. (2011)
	TRGO with AuNPs	~ 0.2 ng/mL	_	0.2 ng/mL – 0.2 mg/mL	CDC	IgG	Mao et al. (2011)
	Vertically-aligned CNT	_	[a]33 μA/(μM mm^2)	100 nM – 1000 nM	CDC	Thrombin protein	Jr et al. (2011)
	PPy-NDFLG	100 fM	[b](S/N = 3.1)/ [c] > 1 s	10 fM - 10 nM	CDC	VEGF RNA aptamer	Kwon et al. (2012)
	Nanowire	>200 pM (depends on high surface = 7.3×10^{11} IgG molecules / cm^2)	[a]high sensitivity at1.35 fM (50 fg/mL cTnT)	20 pM – 4.7 nM	CDC and voltage	cTnT and cTnI by reduced antibody (whole IgG, $F(ab')_2$, Fab antibody)	Elnathan et al. (2012)
	Plasma-treated bilayer graphene	0.04 fM	[b](S/N = 4.2)/[c] >1 s	0.04 fM – 400 pM	CDC	Odorant, amyl butyrate (AB)	Park et al. (2012)
	Vertically-aligned Zno nanorods	~ 0.05 μM	[a]10 μA cm^{-2} mM^{-1}/ [b] 5.2	0.001 mM – 45 mM	CDC	Electroactive species, human serum (H4522) and blood sample	Ahmad et al. (2013)
	Si-nanograting	>10 fM	_	1fM – 1nM	CDC	Insulin in serum	Regonda et al. (2013)
	Non-nanomaterials	12.0 nM	_	15.2 – 1040 nM	CDC	Lysozyme	Goda and Miyahara (2013)
	Non-nanomaterials	6.7 nM	_	13.4 - 1300 nM	CDC	Thrombin	Goda and Miyahara (2013)
	Enzyme-coated ZnO Nanowire	>1 pM	[c] ~ ms/[d] change up to 227 nS (14.7 nS of conductance increase with uric acid)	1pM – 0.5 mM	CDC	Uric acid (UA)	Liu et al. (2013)
	MoS_2 without HfO_2	1 pg/mL	_	1 pg/mL	CDC	Prostate specific antigen (PSA)	Lee et al. (2014)

				– 10 ng/mL			
	MoS_2 with HfO_2	_	[a]196 at 100 fM	10 µM – 100 fM	CDC	Specific protein (SpA)	Sarkar et al. (2014)
	CVD graphene	11 pM	_	100 pM - 580 pM	CDC	Poly-l-lysine	Kakatkar et al. (2015)
	Non-nanomaterials	>2 nM	_	40 nM – 40 pM	CDC	Prion proteins in blood serum with metal ion (Cu^{2+})	Wustoni et al. (2015)
Other sensors	Zinc oxide (ZnO) Nanowire	_	[d] Increase conductance and mobility ~ 28 cm^2/V.s	0.3 V – 1.8 V	CDC	Remove oxygen species (O^-,O_2^-, O^{2-}) by ultraviolet irradiation	Verma et al. (2008)
	Graphene without platinum nanoparticles (PtNPs)	10 µM	_	10 µM – 300 µM	CDC at gate voltage 0.7 V	For H_2O_2	Zhang et al. (2015)
	Graphene with PtNPs	30 nM	[b](S/N ≥3)	1 µM - 1 mM	CDC at gate voltage 0.7 V	For H_2O_2	Zhang et al. (2015)

[*]CDC, change in drain current; CDSV, change in drain-to-source voltage; CPNTs; carboxylated polypyrrole nanotubes; cTnI, cardiac troponin i; cTnT, cardiac troponin t; CVD, chemical vapour deposition; DSV, drain to source voltage; IgG, immunoglobulin G; N-PANI, nanostructure polyaniline; PPy-NDFLG, polypyrrole-converted nitrogen-doped few layer graphene; PET, polyethylene terephthalate; PVS, poly(vinyl sulfonic acid); SWCNT, single-well carbon nanotube; TRGO, thermally-reduced graphene oxide; VEGF, vascular endothelial growth factor.

3.2. Silicon nanowire-based FET biosensors

NWs, especially silicon NWs (SiNWs), are attracting researchers' curiosity due to their unique electrical and optical properties. NW crystal rods are in the nanometre range (10-100 nm) and micrometres in diameter with a specific length. These substances may be manufactured from many inorganic materials (Lu and Lieber, 2006; Wu et al., 2002) and are sometimes called nanorods or nanowhiskers. NWs are identified by their basic configuration, such as silicon and germanium (group IV elements), or gallium-arsenide and indium-phosphate (group III-V elements). In SiNW synthesis, size (Wu et al., 2004; Ma et al., 2003), shape (Tian et al., 2009), and doping of SiNWs can be precisely adapted; SiNW fabrication is highly reproducible. For nano-medicine, hypersensitive biosensors may be made from NWFETs by functionalizing the surface (Patolsky et al., 2006a).

Biosensors that employ SiNWs as the transducer and biomolecules as the bio-recognition site can be arranged as a simple FET-based biosensor. Without SiNWs, biosensor devices deplete the current due to poor electric contact between the nanostructure and metal electrodes. Therefore, diverse approaches are required to ascertain very good contact between the SiNW nanostructure and metal electrodes. For such a FET-based biosensor, gate sites that are not functionalized with bio-recognizance molecules can potentially participate in non-specific binding resulting in unwelcome noise in the signal. To avoid this problem, a SiNW is used in the gate region of the FET to screen such interactions; such a biosensor has quantitative and selective binding of the target analyte to the receptor on the SiNW surface, which changes SiNW conductivity because the number of charge carriers in SiNWs change by the gating effect of the charged analyte. Various methods for NW configuration were used in biosensors such as flow-assisted alignment, the Langmuir-Blodgett technique, the bubble-blown technique, electric-field-directed assembly, the smearing-transfer method, roll-to-roll printing assembly, and the polydimethylsiloxane (PDMS) transfer method (Chen et al., 2011). The development of the Si-NWFET drew in sensor networks (Patolsky et al., 2007). Examples of SiNW-based FET biosensors are discussed in the following sections.

3.2.1. pH sensors. The first use of the SiNW FET device to detect the analytes via solution pH occurred in 2001 (Patolsky et al., 2006b). Oxide-coated SiNW FET with functionalized siloxane acids have a comparatively strong sensitivity to pH and, with different biological receptors, can selectively detect biological entities in solution (Cui et al., 2001). The use of SiNWs for pH biosensing was demonstrated by Pao-Sah integral after applying a parabolic potential estimation to Poisson's equation in the cylindrical coordinate system in a depletion model of a SiNW-based pH sensor. The SiNWs were functionalized with a surface oxide layer that contained amino (NH_2) and silanol (SiOH) groups. This biosensor was comprised of three regions: an insulating native oxide layer, a cylindrical SiNW, and an electrolyte solution that comprised the target molecules. To ensure very good electrical con-

tact between the SiNW and the metal electrode surface oxide layer paste was applied to the SiNW. Short-channel and quantum effects were not shown in this proposed model (Yu, 2014).

3.2.2. Protein sensors. Regonda et al. demonstrated a new FET-biosensor based on Si nano-grating (SiNG) for the selective detection of an insulin-analogue in buffer solution and diluted human serum. It had a detection limit of less than 10 fM (Regonda et al., 2013). Puppo et al. fabricated a protein sensor using a SiNW in the gated micro region. These SiNWs were functionalized with glycidoxypropyltrimethoxysilane (GPTS)-attached anti-rabbit antibody against bio-analytes in tumor extracts in 10 mM ethanolamine solution, deposited on to the SiNW surface because the remaining active GPTS groups were blocked. The GPTS groups with anti-rabbit antibody were deposited on to the microfabricate gate electrodes to fabricated the biosensor with multiple SiNWs connected between the source and drain electrodes. This device detected exogenously added rabbit antigen in a human breast tumor extract, i.e., a much more complex environment, in the range 5-200 fM on a single NW. A SiNW-based device was previously reported for the detection of pathogenic factors at very low concentrations (fM) in phosphate buffered saline (PBS). In this device, the SiNW senses rabbit antigen molecules in the presence of a 100 000 mass excess of the non-specific tumor protein, indicating that the biosensor is excessively resistant to noise (Puppo et al., 2014).

Another use of SiNWs was on a silicon-on-insulator (SOI) substrate in a square-wave structure with the hydroxyl groups to forming a tripod shape at the gated area of the FET; these SiNW structures are superior to the linear structure for biosensing applications due to the large wider reactive surfaces. Afterward, the SiNWs were incubated in a solution of 1 mg/mL NH2−poly (ethyleneglycol) (PEG) in PBS buffer solution and then nonspecific binding to the SiNW surface was eliminated. The tail group of the tripod shape was attached to the amine-functionalized biomaterials because all the peptides contained an amine group on the N-terminus. Further, the artificial peptide-modified Au nanoparticle complexes were connected to the SiNW surface and then detected Matrix Metalloproteinase-2 (MMP-2). In this device, Au nanoparticle complexes perform an important role by increasing sensitivity through a high conductance value, which amplifies the decreasing conductance signal when MMP-2 is applied to the device. This method is preferable to an immune reaction-based FET biosensor from a practical viewpoint, because it is a non-labeling system with one-step reaction kinetics, and it does not require the use of untenable and costly antibodies. Hence, Au nanoparticle complexes enhanced the sensitivity by 10-fold relative to the peptide alone (Choi, et al., 2013). Wang et al. Suggested attaching Ab1 to the surface of the SiNW FET device to detect negatively-charged adenosine triphosphate (ATP) (Wang et al., 2005). SiNWs devices were used by Hahm and lieber (2004) to detect single-stranded DNA. In this device, peptide nucleic acids (PNAs) were used as the receptor because the uncharged PNA molecules have greater affinity for and stability with corresponding DNA recognition sequences at low ionic strength.

Using the bio-recognition layer entrapment method in the gated region of the FET, such as used by Gao et al. (2010), demonstrated that the sensitivity of the NW-FET biosensor can be rapidly enhanced in the sub-threshold regime because the gating effect of bound molecules on a surface is more effective for reduced charge carriers in NWs. Elnathan et al. (2012) reported that we can directly detect bio-molecules in untreated serum, based on the fission of antibody-capturing units; a bio-recognition event could fall in closer proximity to the surface of the NW and the charge could fall within the Debye screening length on the surface. Full antibody, $F(ab')_2$, and Fab fragments attached through-free amine groups or lysine residues on the FET surface for analysis of cardiac troponin t (cTnT) and cardiac troponin i (cTnI) were attached by a glutaric dialdehyde cross-linking step. These fragments are very small receptors, and more methods are utilizing a new generation of small receptors, such as the light chain of the antibody (Masa et al., 1994) used alone or single-chain Fv (Glockshuber et al., 1990). Thus, reducing the ionic strength increases the detection sensitivity for biological entities and chemicals.

3.3. Titanium dioxide-based FET biosensors

Nanostructure sensor fabrication consists of several semiconducting materials, such as 1-D titanium dioxide (TiO_2) materials. TiO_2 NWs in gas sensors and immunosensors have acceptable sensitivity for humidity, hydrogen gas, and Listeria monocytogenes (Li et al., 2010a; Varghese et al., 2003; Wang et al., 2008). TiO_2 is a very interesting component in nanomaterials due to its wide energy gap (between 1.8eV and 4.1eV), which gives a good sensitivity range compared to other materials for biosensing FETs (Wang et al., 2008). In addition, 1-D TiO_2 can be easily manufactured with stable photochemical and chemical properties (Li et al., 2010b; Bao et al., 2008).

3.3.1. pH sensors. Recently, Guerra and Mulato investigated a pH sensor based on titanium oxide nanorods (NRTiO) in the pH range of 2-12, with a sensitivity of 49.6 mV/pH. Voltammetry data presented a sensitivity of 47.8 mV/pH (Guerra and Mulato, 2014). Rosdan et al. suggested that the TiO_2/ITO glass presented the good sensitivity of 42.1 mV/pH and linearity of 0.9997 in the dynamic range of pH4, pH7, and pH10, which was more excellent the bare ITO glass sensitivity of 31.3 mV/pH and linearity of 0.9868 (Rosdan et al., 2013). Vieira et al. suggested that a low-cost separative extended gate FET (SEGFET) pH sensor can be easily made by the layer-by-layer (LBL) technique. Poly (propylene imine) dendrimer (PPI) and TiO_2 nanoparticles were put onto the gold-covered substrates for easily detecting the pH value. Firstly, PPI/TiO_2 was enlarged on an Au or quartz surface upon submerge in the polycationic PPI solution followed by immersion in anionic TiO_2 solution. Further, the PPI/TiO_2-films were immersed in various buffer solutions to measure the pH sensitivity and then ordered to maintain a standard sensitivity of ca. 57 $mVpH^{-1}$ in the range of pH 4 to 10. In this device, the amphoteric oxide surface could show chemical species in three forms, i.e., neutral (AOH), negatively (AO^{--}), and positive (AOH_2^+) charged groups. The H^+ ion changes in the solution lead to changes in the oxide surface potential. In addition, the advantages of this device are that it will be reusable and, importantly, the transducer is isolated from the environment (Vieira et al., 2012).

Another demonstrated use of monomer (Pa) utilised the electro-polymerization of polypyrrole propylic acid (PPa) film on to the patterned TiO_2 NW surface for an abutment reaction. The initiative step was agglutination of TiO_2 NW by using the hydrothermal method onto the exposed gated micro region. After electrochemical polymerization (ECP), PPa/1° Ab film covered the TiO_2 NW surface NW by the cyclic voltammetry method. ECP Pa has large affinity for encapsulating biomolecules in the sub-micro scale and this can be expected to increase the sensitivity of the device. When 11.9 ng/mL of 2° Ab was added to the PPa/1° Ab-coated device, significant increases in I_D were then measured before and after ECP of PPa/1° Ab, compared to the PPa-only group. In this study, the anti-rabbit immunoglobulin G (IgG) (1° Ab) was attached to the TiO_2 NW to especially capture target rabbit IgG (2° Ab), and the PPa-coated TiO_2 NWs-based FET attended as a rein group. Therefore, in concentrations ranging from 119 pg/mL to 5.95 ng/mL, the limits of detection were -3.96 A/(ng/mL) at 5V of the applied V_{DS} and R-square = 0.903. In this fabricated sensor, the encapsulation of the biomolecules by the electrochemically polymerized pyrrole propylic acid was used for the easy detection of anti-rabbit antigen (Chu et al., 2011).

3.4. Zinc oxide nanowire-based FET biosensors

In today's era, work on SiNWs and carbon nanotube-based FET is progressing very quickly. Because the volatile SiNW surface can be oxidized too easily, this may depreciate the device's reliability and sensitivity (Bunimovich et al., 2006); this problem can be avoided by use of a zinc oxide nanowire (ZnO-NW). ZnO-NW have the best electrical properties and biocompatibility for biosensing (Zhao et al., 2009; Zhou et al., 2006), showing great promise because of their adjustable properties, such as semiconductor activity (band gap of 3.37 eV), bio-safety, piezoelectric capability, and bio-compatible nature (Ahsanulhaq et al., 2009; Hahn, 2011; Umar et al., 2008). ZnO-NWs can easily absorb low isoelectric point (IEP) or enzyme proteins (Chox, IEP¼ 4.9) with its extraordinary IEP (9.5). ZnO-nanorods matrices are positively charged, can support a compatible microenvironment for negatively-charged proteins or enzymes, and can improve direct electron transfer between the enzyme and the electrode to a great extent (Zhang et al., 2004; Wang et al., 2012). ZnO-NW was fabricated into the biosensors for real-time detection of bio-species. A biosensor employing ZnO-NWs as the transducer and biomolecules as bio-recognition phenomenon constructs was used as a simple FET sensor. Furthermore, ZnO nanorods or NW-based FET can also exhibit superior electron mobility, up to 1000 cm^2/Vs (Park et al., 2004). Hence, various approaches have to ascertain good contact between the ZnO-NWs and the metal electrode in the FET biosensors. For such a biosensor, NW sites that are not functionalized with bio-recognition molecules can potentially partake in non-specific binding, resulting in vexed noise in the signal; to avoid this problem ZnO-NWs are used to screen such contacts. Examples of ZnO-NW-based FET biosensors are discussed in the following sections.

3.4.1. Cholesterol sensor. Ahmad et al. fabricated a cholesterol sensor using the vertically-aligned ZnO nanorods (ZnO-NRs) grown discriminating on the pre-patterned substrate in solution. ZnO-NR arrays were first used directly on Si/SiO_2 by site-selective growth of the nanorods by the solution process and enzyme solution was prepared by dissolving ChOx. This solution was coagulated on to the surface of ZnO-NRs by physical adsorption. Further, cholesterol was immobilized on the surface of ZnO-NWs and current was substantially enhanced from lower to higher concentrations (i.e., 0.001 to 45 mM) at room temperature. Therefore, the fabricated sensor showed a high sensitivity of 10 µA cm^{-2}

Mm^{-1} and a limit of detection of ~ 0.05 µM. The stability of the fabricated sensor was demarcated by repetitive measurements one day for 6 weeks. This biosensor showed high stability for the detection of cholesterol, which was about 95% of its real response to cholesterol after 30 days of collection; the current value of the sensor was decreased by ~ 12% and ~ 35% in human serum and whole blood samples respectively (Ahmad et al., 2013).

3.4.2. Uric sensor. The use of the enzyme-coated single ZnO-NW-based FET for biosensing was demonstrated by using a chemical vapour deposition (CVD) furnace without any catalysts for the detection of uric acid (UA). First, ZnO-NW was handled by oxygen plasma to remove contaminants and hydroxyl groups were immobilized to the surface of the NW. Further, the NW was dipped in a 2% ethanol solution of 3-aminopropyltriethoxysilane (APTS). After bonding, 5 µL uricase was cast off on the surface of the ZnO-NWs and the device was saturated by glutaraldehyde vapor. In this sensor, bovine serum albumin (BSA) (10 mg/mL) was deposited for two main reasons: first, BSA blocked the unchanged site to reduce the nonspecific binding interplay, which can remove the negative results and hence decrease the ratio of signal to noise; second increase the concentration of protein can bestead to put the enzymatic activity of uricase. Furthermore, when the BSA was added to the NW the baseline re-equilibrated to a minimum value, whereas UA was deposited into the solution in the range of 1 pM to 0.5 mM, with the concentration increased tenfold every time because one UA keeps two hydrogen ions and thus alters the hydrogen ion activity of the solution. This fabricated sensor was much more sensitive at low UA concentrations than high concentrations. When 300 µM lactate and 300 mM glucose were deposited on the NW, the signal was altered only slightly because this sensor enzyme catalysis reaction is very special due to the uricase functionality (Liu et al., 2013).

Another physical method to change the conductance of ZnO-NWs surfaces was modified to enhance immobilization efficiency; the cross-linking method was widely used instead of physical absorption (Choi et al., 2010). Verma et al. demonstrated that conductance of the ZnO-NWs increased approx. 17 times by using ultraviolet irradiation treatment at high temperature under vacuum. Mostly, ZnO-NW absorbs oxygen molecules in the form O^- and O^-_2 from the atmosphere at very high temperature (>450 K) and O^{2-} at room temperature by accepting the electron from the conduction band. The ZnO-NWs comprise the great number of surface oxygen sites due to the very large surface-to-volume ratio. According to this phenomenon, the surface electron depletes from the surface of the ZnO-NW and hence decreases the channel conductivity. Further, ZnO-NWs can increase the conductivity due to the reduced density of parasitic gaseous molecules by the very large vacuum and temperature; mainly, oxygen species, such as O^-, O^-_2 and O^{2-}, engaged the dangling bond on the ZnO-NWs, resulting in depletion layer thickness decreases and conductive channel diameter increases in the NW. In the ZnO-NWs, a valuable increase in the current occurred by UV radiation linked with annealing and high vacuum treatment propounds that UV radiation aid in unseating the tight bonds of the oxygen species to the ZnO-NW surface. UV irradiation readily breaks the oxygen molecules bound to the ZnO-NW surface due to the high energy (>3.2 eV), as the heat of the chemisorptions of the oxygen on the oxides is only of the magnitude of 1.0 eV. Because of this phenomenon, an electron-hole pair is created on surface of the NW and then current values increase from ~ 0.4 µA to ~ 7 µA at the bias voltage of 3V (Verma et al., 2008). However, this kind of detection method requires integration with optical instruments to interpret binding phenomena success into a readable signal (Chen et al., 2011), making the sensing measurement costly. Thus, graphene-FET based biosensors can be suitable for UA analysis, relative to other biosensing devices.

3.5. Gallium Nitride Nanowire-based FET biosensors

During the last two decades NWs and nanotubes were made from a wide class of nanomaterials have showed good electronic, mechanical, and chemical characteristics. Gallium nitride (GaN) NWs show promise due to an instinctive large band gap, coupled with structurally-created electronic and optical imprisonment (Ayres et al., 2006). Alur et al. suggested that the AlGaN/GaN surface was used as a sensing platform in FET due to a high electron mobility transistor (HEMT) wafer with a 2DEG mobility of 1300 cm^2/v-s and a charge carrier density of 1×10^{13} cm^{-2} in sheet. Further, DNA was immobilized on the Au surface in the gate region and then was carried out using thiol group in this device. Hence, it is possible to easily detect DNA using an AlGaN/GaN HEMT biosensor (Alur et al., 2009). Podolska et al. suggested that an AlGaN/GaN-based FET biosensor has very large potential to detect the analytes compared to the Si-based FETs due to AlGaN/GaN high thermal and chemical stability in solution and good compatibility with living cells (Podolska et al., 2013).

Recently, Podolska et al. fabricated the label-free AlGaN/GaN-based FET biosensor for the detection of live cell biological activity. In this fabricated sensor, first, a live cell was confined to the gate

micro-region of packaged AlGaN/GaN NWs and subsequently exposed to different chemical changes in the solution. The biological signal was induced by cell depolarisation with KCl. Biological activity and selectivity were developed by buffering solution with 30 mM 4-(2-hydroxyethyl)-1- piperazineethanesulfonic acid (HEPES). Further, reproducible calcium concentration-dependent reactions were enabled by keeping calcium at the simple physiological level of around 2.5 mM. Before calcium dosing, live cells were pre-deported without calcium solution in isolated experiment with calcium channel blockers, Nisoldipine and Mibefradil, and calcium channel activators, S-BayK(-)8644 and HC-030031. Finally, the resulting signal was compared to the depolarization-induced calcium intake and physiologically-relevant calcium ion channel behaviour (Podolska et al., 2013).

Chen et al. fabricated a DNA sensor using a GaN-nanowire based on an extended gate FET biosensor to detect the human p53 tumor-suppressor gene via label-free, real-time measurement. Firstly, before the immobilization of probe DNA varieties on the GaN surface, pristine GaN was hydroxylated in acidic solution at room temperature. Then, the GaN surface was converted to (3-mercaptopropyl) trimethoxysilane (MPTS) in methanol solution and this surface also exhibited the positive shift (I_D-V_{RE}) in the existence of negatively-charged thiol groups. The Modified MPTS-GaN surface was incubated in the probe DNA solution to immobilize the DNA probe onto the surface. In this device, importantly, a lower detection limit was easily achieved, ~ 6 orders lower, in the detection range 10^{-19}–10^{-6} M and sensitivity was ~ 2 orders higher than GaN thin film-extended gate FET. GaN thin film-based biosensors are very good due to detection limits at approx. the picomolar level, in the dynamic range 10^{-12}–10^{-6} M. Thus, GaN NW-based extended gate FET plainly outperformed its thin film counterpart, revealing the significant potential of NW-based biosensor and bioelectronics applications for detecting various classes of biomolecules (Chen et al., 2011).

3.6. Carbon nanotube-based FET biosensors

Recently, carbon nanotubes (CNTs) have been thought to be promising carbon-based nanoelectronic devices. CNTs are made from one or more layers of graphite, complemented by fullerenic hemispheres that coextend with hollow cylindrical tubes. Effective layers of CNTs were tested in biosensors with different device architectures and designs of construction. CNTs allow a more suitable environment for immobilized biomolecules and hence provide fast electron movement with the electrode surface (Pourasl et al., 2014). Mostly, CNT-based electronic devices are used for detection of various bio-molecules. CNT-based electrochemical sensors (Vashist et al., 2011; Vashist and Venkatesh, 2012) were used to detect bio-molecules, such as glucose, neurotransmitters, cells, DNA, proteins, and microbes, due to the fast response and the most extreme possible values of detection.

Biosensors employing a CNT as the transducer and biomolecules as a bio-recognition site can be configured as a chemiresistor sensor. For such a biosensor, nanomaterial sites that are not functionalized with the various biomolecules can potentially take part in non-specific binding, resulting in undesired noise in the signal. To avoid this problem, CNTs are used to screen such interactions. A CNT-based FET has many applications and is very useful in electronic devices for chemical functionalization of CNTs. The CNT surface acts as an acceptor for hydroxide ions (Lee et al., 2007) on the FET; ilustrative examples of the above phenomenon are discussed in the following sections.

3.6.1. Glucose sensors. Many groups have demonstrated that CNT-based glucose sensors exhibit very high sensitivity, reproducibility, and selectivity. Pourasl et al. reported that detection of glucose is analytically modelled in the CNT-based FET biosensor and the concentration of glucose operates as a function of gate voltage. According to this model, two main approaches of analytical modelling can be used in CNT-based FET biosensors: a charged-based framework and a non-charged framework using the surface-potential-based analysis method. CNT-based glucose sensors show good sensitivity (18.75 A/mM), with a linear range of 2 to 10 mM at drain voltage 0.7 V. Due to the oxidation of H_2O_2 and good quality of the applied polymer substrate, one can keep immobilized GOx in the potential range of 2 to 50 mM; however, the normalized root mean square (RMS) error is present (13% on average) but does not increase in this model. The difference between experimental and simulation values was due to the onset of saturation impression in the drain current at very high gate voltages and because the enzyme response was limited in the used glucose concentrations (Pourasl et al., 2014).

Another demonstrated use of nanohybrids of carboxylated polypyrrole (C-PPy) nanotubes was wrapping them with a graphene sheet to fabricate the transducer in a FET biosensor. This composite, namely reduced graphene oxide (rGO)/C-PPy, was selected for the powerful π-π interactions between PPy nanotubes and graphene sheets. This biosensor shows the Ohmic contacts in the gate region and between the molecules and electrodes. Its conductivity was greater than that of graphene or C-PPy nanotubes in disseverance and provided an emphatic electrical platform between the C-PPy

nanotubes and graphene, then inducing decreased resistance in the resistance of composites. In this biosensor, drain current is increased at various gate voltages ranging from -1V to 1V, due to the highly negative gate of FET. This phenomenon is presented in a p-channel transistor and hence we deduced that the drain current increased due to the hole transport and that changes of drain current resulted from reining the hole concentration at the surface of the composite. The oxidation of glucose works in the fabricated biosensor through the following reaction:

$$\beta\text{-D- glucose} + O_2 + H_2O \longrightarrow \text{D-glucose-1,5-lactone} + H_2O_2 \quad (1)$$

$$H_2O_2 \longrightarrow O_2 + 2H^+ + 2e \quad (2)$$

GOx was used as a glucose target probe in this fabricated biosensor and tightly attached onto the composites through a chemical coupling reaction. The effect of the equations (1) and (2) that propels indirect p-type doping effects results from direct electron transfer through oxidation in the graphene and C-PPy nanotube backbone. This biosensor exhibited very good sensitivity to the glucose signal, with a limit of detection of ~ 1 nM (S/N = 3.22). The biosensor had remarkable changes in the current when glucose was filled in the solution chamber, even at very low concentrations, compared to UA and ascorbic acid (AA) in the analyte (Park et al., 2015). Carboxylated polypyrrole nanotubes (CPNTs) are fabricated by chemical polymerization of an intrinsically functionalized pyrrole–3–carboxylic acid (P3CA) via covalent linkages on the gated area of the fabricated FET biosensor. GOx attaches to CPNT by covalent binding and functionalization of covalent binding provides excellent thermal stability and enzyme activity. Thus this fabricated FET-based biosensor provided a highly sensitive, real-time response (an increase in source to drain current) for the detection of glucose in range of 0.5–20 mM, i.e., it had a very high sensitivity of 1.7. However, this sensor had insignificant responses up to 10 mM in response reveal to gluconic acid (Yoon et al., 2008).

3.6.2. Protein sensors. First, the dense networks of carboxylated vertically-aligned single-walled nanotubes (SWNT) on the FET were made from aged dispersions of shortened SWNTs dispersed in dimethylformamide (DMF) (Chattopadhyay et al., 2001). The vertically-aligned CNTs were successfully fabricated in the gated Si-based metal oxide semiconductor FET for high-performance thrombin detection, based on thrombin aptamers. Further, ssDNA was modified at 3' end, with amine groups attached via covalent binding of thrombin aptamers to the carboxyl removed SWNT. When 1-(3-dimethylamine) propyl)-3-ethylcarbodiimide hydrochloride (EDC) acts with the carboxyl groups of SWNT to generate an effectual ester intermediate, an amine nucleophile that permits amide bond formation between the SWNT and thrombin aptamers. These samples were tested with the surfactant sodium dodecyl sulphate (SDS) in phosphate buffer solution (PBS), because ssDNA oligonucleotides assumed a vertical shape and alleviated the nonspecific binding of the thrombin aptamers to the SiO_2 surface. Due to increasing thrombin concentration, the drain current linearly increased in an aqueous environment (pH = 5.5), then resulted in thrombin sensitivities as high as 33 μA/(μM mm^2) (Jr et al., 2011). Coating nanotubes with polyethylene imine (PEI) or poly (ethyleneglycol) (PEG) polymers changes the characteristics of the FET from p- to n-type; this is used for binding nonspecific proteins (e.g., streptavidin) and receptors (e.g., biotin) to the nanotube sidewalls, attached at room temperature in a15 mM DMF solution of biotin–N–hydroxysuccinimide ester. These sensors are very active, fast, and small enough to detect viruses or individual proteins (Star et al., 2003).

Another physical method to change the conductance of CNTs was used by Byon and Choi who reported that non-specific and specific proteins, such as *Staphylococcus aureus* (SpA), streptavidin (SA), and SpA by IgG and human chorionic gonadotropin (hCG) by anti β-hCG pairs, respectively, can be easily detected by the increased Schottky contact area of the FET biosensor (Byon and Choi., 2006). In the gas phase, the device responds via charge transfer between the conducting nanotube channel and the analyte. As proof, in these experiments, NH_3 molecules donated electrons and withdrew NO_2 molecules (Kong et al., 2000). In 1991, Hansch checked the nanotube FET (NTFET) characteristics when molecules such as anisole, toluene, nitrobenzene, chlorobenzene, phenol, and aniline were immobilised on the NTFET surface. These compounds non-covalently bind to CNTs and change its inductance and resonance. The ascending order of electron donation is NH_2 > OH > OCH_3 > Cl > NO_2 (Hansch et al., 1991). The device's characteristics were changed drastically when the air-dried aromatic compound was a drop (1 nm resolution) on the NTFET device. So, we have to solve for the same concentrations of these compounds exposed to the NTFET devices, the device characteristics when measured in solution, and the important roles these play in the NTFET device. The gate voltage is shifted when charge moves between the aromatic molecules and the NTFET device (Hansch et al., 1991). Gate voltage shifts correlated with the σ_P values and a linear positive relation was observed between the Hammett values and the gate voltage shift. Consistent with the presence of electrons in the ambient conditions on the device are withdrawals of the O_2 species (Tans et al., 1998; Hansch et al., 1991); however, controlling the diameter of the CNT is critical because the FET's

electrical characteristics strongly depend on the CNT's diameter and metal work function (Ohno et al., 2010a).

3.7. Graphene-based FET biosensors

Graphene was discovered in 2004. Recently, graphene is used extensively in nanomaterials (Dresselhaus and Araujo, 2010; Vashist and Venkatesh, 2013b) and is one of the most exciting nanomaterials in biosensors (Zhu et al., 2010). In fact, a single layer of graphene is the honeycomb lattice of the carbon atoms arranged in a two-dimensional array; graphene has earned much attention in its one- and two-dimensional forms (Chowdhury et al., 2011) due to its very high surface area (2630 m^2/g vs. 342 m^2/g for porous SiNW), high thermal (~ 5000 W/mK) and electrical conductivity (550 S cm^{-1}), good strength (Zhu et al., 2010; Teymourian et al., 2013; Cai et al., 2014), and mechanical strength (Young's modulus ~ 1100 GPa) (Lee et al., 2008). The semiconductor gap of graphene is zero in the conduction band and the valence band is at the K–point (Ohno et al., 2010a). The carrier mobility is excessively high for a single layer of graphene at room temperature (~ 2 m^2/Vs vs. 30-560×10^{-4} m^2/Vs for SiNW) (Geim and Novoselov, 2007; Novoselov et al., 2004; Cai et al., 2014). Furthermore, graphene oxide (GO) also exhibits exceptional optical, electrical, chemical, and mechanical properties related to resonance energy transfer for the detection of cysteine (Cys), proteins, metal ions (Gao et al., 2014), negatively-charged bacteria, DNA hybridization, and immunoglobulin E (IgE) graphene (Kuila et al., 2011) in various types of biosensors. The large mobility and surface area of graphene suggests that this nanomaterial has potential for application as a biosensor. Biosensors and electrochemical sensors, such as graphene-based enzyme biosensors, graphene-based electrochemical DNA biosensors, and graphene-based electrochemical sensors for heavy metal ions, have been used for high biosensing and have had very good performance (Shao et al., 2009).

Graphene is employed as a transducer and a bio-recognition site in fabricated biosensors. To alleviate graphene's and GO's many problems, graphene and GO are used to monitor such interactions in FET. Such a biosensor, upon binding of the analyte target to its receptor in graphene and GO, then shows the change in conductivity of graphene and GO, due to the charge carrier's change in the graphene and GO surface brought about by effect of gating of the charge analyte. The biosensing device based on graphene was sufficiently biocompatible to be used in situ and indicated the dye-labeled DNA for optical testing (Vashist, 2013a). Graphene-based FET biosensors depend on two important considerations: the Debye length and functionalization of the receptor without defects on the graphene surface to enable specific detection and minimize nonspecific binding (Ohno et al., 2010b). Illustrative examples of the above phenomenon are discussed in the following sections.

3.7.1. DNA sensors. Kakatkar et al. reported a CVD graphene-based FET biosensor used for the detection of double-stranded DNA and poly-l-lysine. The Dirac voltage was shifted due to the binding or nonbinding of charged biomolecules with the CVD graphene surface. The response of the polarity changes due to poly-l-lysine were positive and those due to DNA were negative (Kakatkar et al., 2015). Ohno et al. also reported that a graphene FET biosensor can easily detect positively and negatively-charged protein (i.e., BSA), while CNT-based FET biosensor can only detect positively charged biomolecules (Ohno et al., 2010a). Cai et al. demonstrated a new fabricated biosensor based on reduced graphene oxide (R-GO) for the label-free detection of peptide-nucleic acid (PNA)-DNA hybridization. First, R-GO was fabricated onto the sensor chip by the drop-casting method and then PASE (a linker molecule) was attached to the surface of R-GO by π-π stacking interactions between the pyrene and graphene surfaces. Further, a PNA probe was deposited via covalent bond between the amino group and PNA, the amide bond was attached to the other end of PASE, and ethanolamine solution was used to alleviate the nonspecific binding. Finally, the target DNAs were immobilized onto the channel for hybridization with the PNA probe. Hence, this fabricated sensor had a detection limit of less than 100 fM. In contrast, reusability was checked by three cycles of the hybridization and dehybridization. After finishing the three cycles, the second and third hybridization signals were 96.67 and 83.33% of the first hybridization signal, respectively, and noise level ~ -12 mV from the blank control test (Cai et al., 2014). Polymer, such as polypyrrole converted into nitrogen-doped graphene, is grown on the Cu surface by CVD, combined with vapour deposition polymerization for detecting vascular endothelial growth factor (VEGF) RNA aptamers. The detection limit was ~ 100 fM and the sensitivity decreased (<5%) after 20 cycles (Kwon et al., 2012).

3.7.2. Protein sensors. Lu et al. suggested that His-tagged proteins are easily detected by graphene FET (G-FET) biosensors by the binding of Ni ions to the nitrilotriacetic acid (NTA) (Lu et al., 2012). FET based on aptamer-modified graphene easily detected the IgE protein because the reaction be-

tween IgE aptamers and IgE protein is highly active; the solution was stirred for several tens of seconds after the addition of each analyte (Ohno et al., 2010b). Odorant and amyl butyrate (AB) analytes were easily detected by using transparent and flexible FETs-a type of bioelectronic-nose. This biosensor was based on the plasma-treated bilayer of graphene modified with oxygen and ammonia plasma treatments to control the band gap. These nanomaterials were conjugated with an olfactory receptor, which attaches to a particular odorant and the detection limit of this sensor with oxygen plasma treatment (p-type) was very low, i.e., 0.04 fM (S/N=4.2), and the sensitivity continuously increased up to concentration of 40 pM. Additionally, the B nose-based biosensor had showed quick response, less than 1s, and the B-nose had good long term stability and could be stored them at 25℃ for 10 days in dry air in a sealed vessel (Park et al., 2012). Mao et al. demonstrated the use of thermally-reduced graphene oxide (TRGO) sheets for specific protein detection and TRGO utilised with AuNPs and anti-IgG in the gated region of the FET. Gold nanoparticles (AuNPs) appeared to be uniformly distributed on the TRGO surface without accumulation. The probe protein was attached to AuNPs by covalent bonding. In this fabricated sensor, blocking buffer (BB) was used to reduce the nonspecific binding of analytes to the device due to undesirable noise in the signal. Further, the fabricated sensor resistance was checked for mismatch; IgM (15.3%) and horseradish peroxidase (HRP) (12.4%) were less than that from the complementary IgG (68.0%). Thus, the modified sheet has many varieties of chemical and thermal processes for detection of various proteins with high sensitivity and low detection limit, i.e., ~13 pM (Mao et al., 2010). Sarkar et al. (2014) suggested that MoS_2-based FET biosensors are more sensitive; with a low detection limit (i.e. 100 fM) for detecting the various bio-molecules, such as biotin, SA, and IgE from mouse serum, compared to some nanomaterials, but not graphene and GO. Because graphene is also a 2D layered material, it shares the same virtues as MoS_2.

3.7.3. Glucose sensors. Zhang et al. demonstrated a new glucose biosensor based on enzyme-modified graphene. First, modified graphene electrodes (with the enzyme GOx) were attached to biocompatible polymers, namely chitosan (CHIT) and Nafion, and also attached to PtNPs by electrochemical deposition due to their enhanced electrocatalytic activity. The sensing mechanism of this fabricated sensor depended on the GOx-catalyzed oxidation of glucose and thus H_2O_2 created the near the surface of the gate electrode. Further, oxidation of H_2O_2 generated the electron on the gate electrode and then sensitivity increased. Hence, the detection limit was 0.5 µM and had more transconductance, 2 mS, than the Si-based FET biosensor, which has only transconducts near 20 µS. The fabricated sensor could not respond with any current when AA its concentration was very low (i.e., 3 µM) (Zhang et al., 2015). Furthermore, Wu et al. investigated GOx/Pt/functional graphene sheets (FGS)/CHIT nanoparticles deposited onto the graphene surface in a FET for glucose detection; it had a detection limit of 0.6µM (Wu et al., 2009). Huang et al. reported the detection of glucose or glutamate molecules by modified redox enzyme (GOx or glutamic dehydrogenase (GluD)) immobilised on the CVD-grown graphene sheet via linker molecule (1–pyrenebutanoic acid succinimidyl ester) in 10 mM PBS solution of pH 7.2. It is a very expensive reaction to increase the conductance of the graphene sheet for products from the oxidative reaction; oxidation of glucose and glutamate produced H_2O_2 and NH_4OH, respectively, while graphene conductance did not change after addition of D–glucono-1,5-lactone and -∝-ketoglutarate on the graphene sheet. This fabricated sensor does not respond common interferences, such as UA, L-ascorbic acid, and acetaminophen, and only responded to glucose and glutamate; this indicates that G-FET are better than SWNT-based sensors because the functionalised enzymes are more productive productive and orderly on the level graphene sheet than on small SWNT, and the sensitivity of the SWNT is decreased by the presence of the metallic nanotube (Huang et al., 2010).

3.7.4. pH sensors. Ohno et al. (2010a) investigated bio-chemical sensors using a single-layer graphene-based FET to detect pH values with the lowest detection limit (signal/noise = 3) of 0.025. Ju and Chen reported that nitrogen graphene quantum dots (GQDs) are much better than GQDs for a sensitive response to Fe^{3+} in a broad concentration range of 1–1945µM, with a high detection limit of 90 nM (s/N=3), compared to other sensing devices and can be used as a green and facile sensing platform for label-free sensitive and selective detection of Fe (III) ions in aqueous solution and real water (Ju and Chen, 2014).

Table.2
FET-based biosensor device parameter

length(μM)	Width (μM)	SiO_2/Si (nM)	Ti(nM)/Au(nM)	Nanomaterials	detection	Detection limit	References
0.75	_	200	35/5	Nanotube	SA	_	Star et al. (2003)
700×10^{-3}	_	100	80/150	ZnO nanowire	Remove oxygen species	_	Verma et al. (2008)
100	30	_	_	SWCNT	Thrombin protein	_	Jr et al. (2011)
1	50×10^{-3}	200	_	TRGO	Protein	~0.2 ng/mL	Mao et al. (2011)
15	_	100	50/150	TiO_2 nanowire	IgG (1° Ab)	-3.96 A/(ng/mL)	Chu et al. (2011)
100	2000	_	_	PPy-NDFLG	VEGF RNA aptamer	100 fM	Kwon et al. (2012)
200	200	300	20/300	MoS_2	PSA	1 pg/mL	Lee et al. (2014)
10	1000	_	_	_	Prion protein	>2nM	Wustoni et al. (2015)
50	_	300	Cr(10)/40	CVD-graphene	DNA and Poly-l-lysine	11 pM	Kakatkar et al. (2015)

4. Comparative Results:

As depicted in Table 1 and 2, various types of nanomaterial based-FET biosensors have been examined on the basis of detection limit, duration of detection, sensitivity, and efficacy. It is evident that pH detection using graphene-based-nanomaterials in FET-based biosensors consists of a very low detection limit and SNR compared to other nanomaterial. Detection of glucose using CPNT-wrapped graphene sheets shows the lowest detection limit with the shortest detection time. Moreover, detection of DNA using rGO nanomaterials has a minimum detection limit in femtomolar range, and detection of protein using PPy-NDFLG and plasma-treated bilayer graphene in the femtomolar range with the shortest detection time reveals that graphene-based nanomaterials are suited for use in FET-based detection devices that require rapid detection. H_2O_2 was detected using graphene with PtNPs by a FET-based biosensor with a minimum detection limit (30 nM). In addition, graphene nano ribbons and graphene QDs are also useful to detect chemical dissolution, with enormous potential for high sensitivity and field effects at the edges; the safety of graphene-based products must be taken into consideration before commercial use. Finally, graphene-based nanomaterials are the best suited nanomaterials for FET-based biosensors for the detection of various biomolecules in terms of detection limit, size, sensitivity, cost, functionality, and high SNR, as shown in Table1. It is also evident from Table 2 that device the fabrication parameters, such as sizes and matrices for the detection of various biomolecules, are excellent (up to femtomolar detection) for few-layered graphene-based composite (Kwon et al., 2012).

5. Conclusion:

This review presents recent advances in the applications of various nanomaterials used for the exposed gated micro-region of the FET for very high electrochemical detection of a vast range of analytes. These nanomaterial-assisted FET-based nanobiosensors have shown very high sensitivity and selectivity for the detection of biomolecules, DNA, protein, electro-active species, human serum (H4522), blood samples, lysozyme, thrombin, and glucose. Based on the characteristics of size, sensitivity, cost, SNR, and ease of fabrication, graphene-based FETs have shown excellent electrocatalytic activity for biosensing and therefore may aid in development of new nanobiosensors. The particular study of graphene on the gated region of the FET will open up new research facets in biosensing but the extent of layering and toxicity must be answered before commercial use.

6. Scope of future work:

Various strategies were explored for the development of novel nano-biosensors that employ carbon-based nanomaterials, like graphene, GO, CNT, and others, as detection elements; the high electrical conductivity and surface areas of the graphene and GO were prepared by various techniques

and can be used to detect the various biomolecules and metal ions. MNPs, AuNPs, and doped graphene can be used to form novel nano-biosensors. The electrochemical achievement of buffer solutions related to graphene can be investigated. Until now, limited research has been carried out on graphene/conducting polymer nanocomposite pastes on the gate of the FET, which can be one of the good nanomaterials for such nano-biosensors.

Acknowledgement:

Authors acknowledge the financial assistance provided by Uttarakhand Council for Biotechnology, Biotech Bhavan, Haldi, U. S. Nagar and Department of Science & Technology, government of India under water technology initiative (WTI).

References

Ahmad, R., Tripathy, N., Hahn, Y-B., 2013. Biosens. Bioelectron. 45, 281-286.
Ahsanulhaq, Q., Kim, S.H., Hahn, Y.B., 2009. J. Phys. Chem. Solids. 70, 627–631.
Alur, S., Gnanaprakasa, T., Xu, H., Wang, Y., Simonian, A.L., Oyarzabal, O.A., Park, M., 2009. CS MANTECH Conference, May 18th-21st, Tampa, Florida, USA.
Artiles, M.S., Rout. C.S., Fisher, T.S., 2011. Adv. Drug Deliv. Rev. 63, 1352–1360.
Ayres, V.M., Jacobs, B.W., Chen, Q., Udpa, L., Fan, Y., Tram, N., Baczewski, A., Kumar, S., Crimp, M., Halpern, J., He, M., Tupta, M.A., Stallcup, R., Hartman, A., 2006. IEEE.
Balasubramanian, K., Burghard, M., 2006. Anal. Bioanal. Chem. 385, 452–468.
Bao, S.J., Li, C.M., Zang, J.F., Chi, X.Q., Qiao, Y., Guo, J., 2008. Adv. Funct. Mater. 18(4), 591-599.
Bergveld, P., 1970. IEEE Trans. Biomed. Eng. 17, 70–71.
Bunimovich, Y.L., Shin, Y.S., Yeo, W.S., Amoro, M., Kwong, G., Heath, J.R., 2006. J. Am. Chem. Soc. 128, 16323–16331.
Byon, H.R., Choi, H.C., 2006. J. Am. Chem. Soc. 128, 2188–2189.
Cai, B., Wang, S., Huang, L., Ning, Y., Zhang, Z., Zhang, G-J., 2014. ACS Nano 8(3), 2632-2638.
Caras, S., Janata, J., 1980. Anal. Chem. 52, 1935–1937.
Chattopadhyay, D., Galeska, I., Papadimitrakopoulos, F., 2001. J. Am. Chem. Soc. 123, 9451–9452.
Chen, C-P., Ganguly, A., Lu, C-Y., Chen, T-Y., Kuo, C-C., Chen, R-S., Tu, W-H., Fischer, W.B., Chen, K-H., Chen, L-C., 2011. Anal. Chem. 83, 1938-1943.
Chen, K-I., Li, B-R., Chen, Y-T., 2011. Nano Today Rev. 6, 131-154.
Choi, A., Kim, K., Jung, H.I., Lee, S.Y., 2010. Sens. Actuators B: Chem. 148, 577-582.
Choi, J-H., Kim, H., Choi, J-H., Choi, J-W., Oh, B-K., 2013. ACS Appl. Mater. Interfaces 5, 12023−12028.
Chowdhury, R., Adhikari, S., Rees, P., Wilks, S.P., 2011. Phys. Rev. B 83, 045401.
Chu, Y.M., Lin, C.C., Chang, H.C., Li, C., Guo, C., 2011. Biosens. Bioelectron. 26, 2334-2340.
Cui, Y., Wei, Q.Q., Park, H.K., Lieber, C.M., 2001. Science 293 (5533), 1289-1292.
Dresselhaus, M.S., Araujo, P.T., 2010. ACS Nano 4, 6297-6302.
Elmore, W.C., 1938. Phys. Rev. 54(12), 1092-1095.
Elnathan, R., Kwait, M., Pevzner, A., Engel, Y., Burstein, L., Khatchtourints, A., Lichtenstein, A., Kantaev, R., Patolsky, F., 2012. Nano Lett. 12, 5245–5254.
Fan, X., White, I.M., Shopova, S.I., Zhu, H., Suter, J.D., Sun, Y., 2008. Anal. Chim. Acta 2008, 620, 8-26.
Fromherz, P., Offenhausser, A., Vetter, T., Weis, J., 1991. Science 252, 1290–1293.
Gao, L., Lian, C., Zhou, Y., Yan, L., Li, Q., Zhang, C., Chen, L., Chen, K., 2014. Biosens. Bioelectron. 60, 22-29.
Gao, X.P.A., Zheng, G., Lieber, C.M., 2010. Nano Lett. 10, 547-552.
Geim, A.K., Novoselov, K.S., 2007. Nat. Mater. 6, 183-191.
Gilchrist, R., Shorey, W., Hanselman, R., Parrott, J., Taylor, C., Medal, R., 1957. J. Ann. Surg. 146, 596–606.
Gleiter., 1989. Prog. Mater Sci. 33, 323.
Glockshuber, R., Malia, M., Pfitzinger, I., Plueckthun, A., 1990. Biochem. 29, 1362.
Goda, T., Miyahara, Y., 2013. Biosens. Bioelectron. 45, 89-94.
Guerra, E.M., Mulato, M., 2014. Mater. Sci. App. 5, 459-466.
Hahm, J., Lieber, C.M., 2004. Nano Lett. 4, 51-54.
Hahn, Y.B., 2011. Korean J. Chem. Eng. 28, 1797–1813.
Hansch, C., Leo, A., Taft, R. W., 1991. Chem. Rev. 91, 165.

Haun, J.B., Yoon, T.J., Lee, H., Weissleder, R., 2010. Wiley Interdiscip Rev Nanomed Nanobiotechnol. 2, 291–304.
Holzinger, M., Goff , A., Cosnier, S., 2014. Front. Chem. 2, article 63.
Huang, Y., Dong, X., Shi, Y., Li, C.M., Li, L.J., Chen, P., 2010. Nanoscale 2, 1485–1488.
Indira, T.K., Lakshmi, P.K., 2010. Int. J. Pharm. Sci. Nanotech. 3(3), 1035-1042.
Janata, J., Moss, S., 1976. Biomed. Eng. 6, 241–245.
Jr, R.A.C, Vaddiraju, S., Chan, P.Y., Seyta, R., Jain, F.C., 2011. Sens. Actuators B160, 154–160.
Ju, J., Chen, W., 2014. Biosens. Bioelectron. 58, 219-225.
Jun, Y., Choi, J., Cheon, J., 2007. Chem. Commun. (Camb) 1203-1214.
Kakatkar, A., Abhilash, T.S., Alba, R.D., Parpia, J.M., Craighead, H.G., 2015. Nanotechnology 26, 125502 (5pp).
Khanna, V.K., 2008. Sens. Rev. 28, 39-45.
Kiani, M.J., Razak, M.A.A., Che Harun, F.K., Ahmadi, M.T., Rahmani, M., 2015. J. Nanomater. 1-7.
Kong, J., Franklin, N. R., Zhou, C., Chapline, M. G., Peng, S., Cho, K., Dai, H., 2000. Science 287, 622.
Koppenhöfer, D., Kettenbaum. F., Susloparova, A., Law, J.K.Y., Vu, X.T., Schwab, T., Schäfer, K.H., Ingebrandt, S., 2015. Biosens. Bioelectron. 67, 490-496.
Kuila, T., Bose, S., Khanra, P., Mishra, A.K., 2011. Biosens. Bioelectron. 26, 4637-4648.
Kwon, O.S., Park, S.J., Hong, J-Y., Han, A-R., Lee, J.S., Lee, J.S., Oh, J.H., Jang, J., 2012. ACS Nano 6(2), 1486-1493.
Law, J.K.Y., Susloparova, A., Vu, X.T., Zhou, X., Hempel, F., Qu, B., Hoth, M., Ingebrandt, S., 2015. Biosens. Bioelectron. 67, 170-176.
Lee, C.S., Kim, S.K, Kim, M., 2009. Sensors 9, 7111-7131.
Lee, C., Wei, X., Kysar, J. W., Hone, J., 2008. Science 321, 385–388.
Lee, J., Dak, P., Lee, Y., Park, H., Choi, W., Alam, M.A., Kim, S., 2014. Sci. Rep. 4, 7352.
Lee, K., Kwon, J.H., Cho, S.M.W.S., Ju, B.K., Lee, Y.H., 2007. Mater. Lett. 61, 3201–3203.
Li, R., Gan, Y., Song, Q.L., Zhu, Z.H., Shi, J.S., Yang, H.B., Wang, W., Chen, P., Li, C.M., 2010a. Nanoscale 2(8), 1474-1479.
Li, Y., Schluesener, H., Xu, S. 2010b. Gold Bull. 43, 29–41.
Liu, X., Lin, P., Yan, X., Kang, Z., Zhao, Y., Lei, Y., Li, C., Du, H., Zhang, Y., 2013. Sens. Actuators B 176, 22–27.
Lowery, T.J., Palazzolo, R., Wong, S.M., Prado, P.J., Taktak, S., 2008. Anal. chem. 80, 1118.
Lu, W., Lieber, C.M., 2006. J. Phys. D: Appl. Phys. 39, 387-406.
Lu, Y., Lerner, M.B., Qi, Z.J., Jr, J.J.M., Lim, J.H., Discher, B.M., Johnson, A.T.C., 2012. Appl. Phys. Lett. 100, 033110.
Ma, D.D.D., Lee, C.S., Au, F.C.K., Tong, S.Y., Lee, S.T., 2003. Science 299, 1874.
Mao, S., Lu, G., Yu, K., Bo, Z., Chen, J., 2010. Adv. Mater. 22, 3521–3526.
Mao, S., Yu, K., Lu, G., Chen, J., 2011. Nano Res. 4(10), 921-930.
Masta, L., Wabl, M., Johnson, J.P., 1994. Proc. Natl. Acad. Sci. U.S.A 91, 893.
Mornet, S., Vasseur, S., Grasset, F., Veverka, P., Goglio, G., A. Demourgues, A., Portiera, J., Pollertc, E., Dugueta, E., 2006. Prog. Solid State Chem. 34, 237.
Novoselov, K.S., Geim, A.K., Morozov, S.V., Jiang, D., Zhang, Y., Dubonos, S.V., Grigorieva, I.V., Firsov, A.A., 2004. Science 306, 666-669.
Ohno, Y., Maehashi, K., Matsumoto, K., 2010a. Biosens. Bioelectron. 26, 1727-1730.
Ohno, Y., Maehashi, K., Matsumoto, K., 2010b. J. Am. Chem. Soc. 132, 18012-18013.
Park, J.W., Lee, C., Jang, J., 2015. Sens. Actuators B 208, 532-537.
Park, S.J., Kwon, O.S., Lee, S.H., Song, H.S., Park, T.H., Jang, J., 2012. Nano Lett.12, 5082−5090.
Park, W.I., Kim, J.S., Yi, G.C., Bae, M.H., Lee, H.J., 2004. Appl. Phys. Lett. 85, 5052.
Patel, D., Moon, J.Y., Chang, Y., Kim, T.J., Lee, G.H., 2008. Colloid Surf., A 91, 313–314.
Patolsky, F., Zheng, G.F., Lieber, C.M., 2006a. Nat. Protoc. 1(4), 1711-1724.
Patolsky, F., Zheng, G.F., Lieber, C.M., 2006b. Anal. Chem. 4261-4269.
Patolsky, F., Timko, B.P., Zheng, G., Lieber, C.M., 2007. MRS Bull. 32,142.
Podolska, A., Hool, L.C., Pfleger, K.D.G., Mishra, U.K., Parish, G., Nener, B.D., 2013. Sens. Actuators B 177, 577-582.
Pourasl, A.H., Ahmadi, M.T., Rahmani, M., Chin, H.C., Lim, C.S., Ismail, R., Tan, M.L.P., 2014. Nanoscale Res. Lett. 9 (33), 1-7.
Puppo, F., Doucey, M-A., Delaloye, J-F., Moh, T.S.Y., Pandraud, G., Sarro., P.M., Micheli, G. De., Carrara, S., 2014. IEEE Sensors, 866-869.
Regonda, S., Tian, R., Gao, J., Greene, S., Ding, J., Hu, W., 2013. Biosens. Bioelectron. 45, 245–251.

Rosdan, M.A., Herman, S.H., Abdullah, W.F.H., Kamarozaman, N.S., Syono, M.I., 2013. Conference: Micro and Nanoelectronics (RSM), IEEE Regional Symposium.
Sarkar, D., Liu, W., Xie, X., Aaron, C., Anselmo, A.C., Mitragotri, S., Banerjee, K., 2014. ACS Nano 8(4), 3992-4003.
Schasfoort, R., Kooyman, R., Bergveld, P., Greve, J., 1990. Biosens. Bioelectron. 5, 103–124.
Schwirn, K., Tietjen, L., Beer, I., 2014. Environ. Sci. Eur. 26, 4.
Shao, H.L., Min, C., Issadore, D., Liong, M., Yoon, T.J., Weissleder, R., Lee, H., 2012. Theranostics 2, 55–65.
Shao,Y., Wang, J., Wu, H., Liu, J., Aksay, I.A., Lina.Y., 2009. Electroanalysis 10, 1027–1036.
Shen, W., Schrag, B.D., Carter, M.J., Xiao, G., 2008. Appl. Phys. Lett. 93, 033903.
Star, A., Gabriel, J.C.P., Bradley, K., Gruner, G., 2003. Nano Lett. 3(4), 459 – 463.
Stevens, P.D., Fan, J., Gardimalla, H.M.R., Yen, M., Gao, Y., 2005. Org. Lett. 7, 2085.
Tans, S.J., Verschueren, R.M., Dekker, C., 1998. Nature 393, 49.
Teymourian, H., Salimi, A., Khezrian, S., 2013. Biosens. Bioelectron. 49, 1–8.
Thevenot, D.R., Toth, K., Durst, R.A., Wilson, G.S., 1999. Pure Appl. Chem. 7, 2333-2348.
Tian, B.Z., Xie, P., Kempa, T.J., Bell, D.C., Lieber, C.M., 2009. Nat. Nanotechnol. 4, 824.
Tian, H., Tan, Z., Wu, C., Wang, X., Mohammad, M.A., Xie, D., Yang, Y., Wang, J., Li, L.J., Xu, J., Ren, T.L., 2014. Sci. Rep. 4, 5951.
Umar, A., Kim, S.H., Kim, J.H., Al-Hajry, A., Hahn, Y.B., 2008. J. Alloys Compd. 463 (1–2), 516–521.
Varghese, O.K., Gong, D.W., Paulose, M., Ong, K.G., Grimes, C.A., 2003. Sens. Actuators B 93 (1-3), 338-344.
Vashist, S.K., 2013a. J. Nanomater. Mol. Nanotechnol. 2, 1-6.
Vashist, S.K., Venkatesh, A.G., 2013b. J. Nanomed. Nanotechol. 4, e127.
Vashist, S.K., Venkatesh, A.G., 2012. J. Nanomed. Nanotechol. 3, e121.
Vashist, S.K., Zheng, D., Al-Rubeaan, K., Luong, J.H.T., Sheu, F.S., 2011. Biotechnol. Adv. 29, 169-188.
Velasco, M.N., 2009. Semin. Cell Dev. Biol. 20, 27-33.
Verma, V.P., Jeon, H., Hwang, S., Jeon, M., Choi, W., 2008. IEEE Trans. Nanotechnol. 7 (6), 782–786.
Vieira, N.C.S., Fernandes, E.G.R., Faceto, A.D., Zucolotto, V., Guimarães, F.E.G., 2011. Sens. Actuators B 160, 312–317.
Vieira, N.C.S., Figueiredo, A., Faceto, A.D., Queiroz, A.A.A.D., Zucolotto, V., Guimarães, F.E.G., 2012. Sens. Actuators B 169, 397–400.
Vijayalakshmia, A., Tarunashreea, Y., Baruwatib, B., Manoramab, S.V., Narayanaa, B.L., Johnsona, R.E.C., Raoa, N.M., 2008. Biosens. Bioelectron. 23 (11), 1708–1714.
Wang, C., Tan, X., Chen, S., Yuan, R., Hu, F., Yuan, D., Xiang, Y., 2012. Talanta 94, 263–270.
Wang, R.H., Ruan, C.M., Kanayeva, D., Lassiter, K., Li, Y.B., 2008. Nano Lett. 8(9), 2625-2631.
Wang, W.U., Chen, C., Lin, K.H., Fang, Y., Lieber, C.M., 2005. Proc. Natl. Acad. Sci. 102, 3208-3212.
Wolf, B., Brischwein, M., Baumann, W., Ehret, R., Kraus, M., 1998. Biosens. Bioelectron. 13, 501–509.
Wu, H., Wang, J., Kang, X., Wang, C., Wang, D., Liu, J., Aksay, I.A., Lin, Y., 2009. Talanta 80, 403-406.
Wu, Y., Fan, R., Yang, P., 2002. Int. J. Nano. 1, 1–39.
Wu, Y., Cui, Y., Huynh, L., Barrelet, C.J., Bell, D.C., Lieber, C.M., 2004. Nano Lett. 4, 433.
Wustoni, S., Hideshima, S., Kuroiwa, S., Nakanishi, T., Hashimoto, M., Mori, Y., Osaka, T., 2015. Biosens. Bioelectron. 67, 256-262.
Yoon, H., Ko, S., Jang, J., 2008. J. Phy. Chem. B 112, 9992–9997.
You, C., Bhagawati, M., Brecht, A., Piehler, J., 2009. Anal. Bioanal. Chem. 393, 1563-1570.
Yu, Y.S., 2014. J. Semi. Tech. Sci. 14(4), 451-456.
Yun, Y-H., Eteshola, E., Bhattacharya, A., Dong, Z., Shim, J-S., Conforti, L., Kim, D., Schulz, M.J., Ahn, C.H., Watts, N., 2009. Sensors 9, 9275-9299.
Yuqing, M., Jianguo, G., Jianrong, C., 2003. Biotechnol. Adv. 21, 527-534.
Zayats, M., Kharitonov, A., Katz, E., Bückmann, A., Willner, I., 2000. Biosens. Bioelectron. 15, 671–680.
Zayats, M., Raitman, O., Chegel, V., Kharitonov, A., Willner, I., 2002. Anal. Chem. 74, 4763–4773.
Zhang, F.F., Wang, X.L., Ai, S.Y., Sun, Z.D., Wan, Q., Zhu, Z.Q., Xian, Y.Z., Jin, L.T., Yamamoto, K., 2004. Anal. Chim. Acta 519, 155-160.
Zhang, M., Liao, C., Mak, C.H., You, P., Mak, C.L., Yan, F., 2015. Sci. Rep. 5, 8311.
Zhao, J., Wu, D., Zhi, J., 2009. Bioelectrochemistry, 75, 44–49.
Zhao, J., Lu, J. P., Han, J., Yang, C-K., 2003. Appl. Phys. Lett. 82, 3746.

Zhao, M., Josephson, L., Tang, Y., Weissleder, R., 2003. Angew. Chem. Int. Ed. 42, 1375.
Zhou, J., Xu, N.S., Wang, Z.L., 2006. Adv. Mater. 18, 2432–2435.
Zhu, Y., Murali, S., Cai, W., Li, X., Suk, J.W., Potts, J.R., Ruoff, R.S., 2010. Adv. Mater. XX, 1–19.

Highlights

►The uses of various nanomaterials in FET-based biosensors are reviewed.
►Graphene-based FET biosensor could be able to easily detect various biomolecules, such as proteins, polysaccharides, cytochrome-c, lipids, NADH, hemoglobin, HRP, nucleic acids, and small molecules, such as primary metabolites, secondary metabolites, and natural products.
►The large surface area and good sensitivity of graphene based nanomaterial in conjunction with polymeric matrices seems to be more beneficial for detecting different biomolecules.